# Differential cross sections for low-energy elastic electron scattering from tetrahydrofuran in the angular range 20°–180°

Marcin Dampc,[1] Aleksandar R. Milosavljević,[2] Ireneusz Linert,[1] Bratislav P. Marinković,[2] and Mariusz Zubek[1]
[1]*Department of Physics of Electronic Phenomena, Gdańsk University of Technology, 80-952 Gdańsk, Poland*
[2]*Institute of Physics, Pregrevica 118, 11080 Belgrade, Serbia*
(Received 22 January 2007; published 18 April 2007)

Absolute differential cross sections have been measured for elastic electron scattering from tetrahydrofuran in the electron impact energy from 6 to 20 eV and in a wide scattering angle range from 20° to 180°. In the measurements the magnetic-angle-changing technique has been employed to detect the backward scattering of electrons. The integral and momentum transfer cross sections for elastic scattering have been also determined through integration of the measured differential cross sections. A detailed comparison of the obtained differential cross sections has been made with the results of very recent theoretical calculations. In the measurements attention has been paid to observe negative-ion resonances predicted in these theoretical calculations.

DOI: 10.1103/PhysRevA.75.042710 PACS number(s): 34.80.Bm

## I. INTRODUCTION

Recent experiments investigating radiation damage in biological systems have clearly established that low-energy electrons ($E \leqslant 20$ eV) induce damage of single- and double-strand breaks in supercoiled DNA with high efficiency [1]. These results prompted extensive investigations of the basic DNA components: namely, the purine and pyrimidine bases, the phosphate group, and the deoxyribose sugar including its simpler analogs of the furanose-structured molecules [2]. Particular attention has been devoted to dissociative electron attachment [3,4] which proceeds via negative-ion resonances. These lead to bond breaking of these building blocks of the DNA molecule which may induce damage in the DNA itself and further result in genotoxic effects. Recently, these investigations have turned to theoretical and experimental studies of elastic and inelastic electron scattering by the above basic DNA components in the gas phase [5,6]. An accurate determination of differential, integral, and total cross sections for electron collisions with the components is important in order to obtain input parameters in Monte Carlo modeling of ionizing radiation energy deposition in human tissue [7,8]. The gas-phase data also play an important role when compared with measurements in solid materials (thin films) in order to learn how the elementary electron processes evolve during the transition from isolated target molecules in the gas phase to many-body interactions in the condensed phase.

In the present work, we have measured absolute differential cross sections for elastic electron scattering from terahydrofuran (THF), $C_4H_8O$. THF can be considered to be a simple analog for the investigations of electron interactions with the deoxyribose ring in DNA and also with the DNA sugar backbone. Our measurements have been carried out using the relative flow technique at the incident electron energies of 6, 7, 8, 10, 12, 15 and 20 eV. These measurements have been performed in a wide scattering angle range from 20° to 180°, applying the magnetic-angle-changing technique [9–11] for scattering into the backward hemisphere from 90° to 180°. We have also determined the elastic integral and momentum transfer cross sections through integration of the measured differential cross sections. The wide angular range of the present experimental cross sections ensures a more accurate determination of these cross sections because it avoids extensive extrapolation up to 180°. In the course of the present work differential cross sections were also measured at fixed scattering angles as functions of incident electron energy with the aim of detecting negative-ion resonances predicted in the very recent theoretical calculations. Preliminary results of the present work have been presented in a conference communication [12].

The studies of low- and medium-energy (<50 eV) electron interactions with THF have attracted considerable attention in last few years and were motivated by research on radiation damage to biological systems. The first absolute differential cross sections for elastic electron scattering from THF have been presented by Milosavljević *et al.* [13] for the energy range from 20 eV to 60 eV measured over the scattering angle range 10°–110°. Very recently absolute elastic cross sections for the lower-energy range from 6.5 eV up to 50 eV that cover the 10°–130° angular range have been measured by Colyer *et al.* [14]. The total cross sections for electron collisions have been reported by Zecca *et al.* [15] at energies at and below 21 eV and by Możejko *et al.* [16] in a wider energy range 1–370 eV. The other existing experimental results for electron collisions with THF include vibrational excitation studies of Lepage *et al.* [17], in both the gas and solid phases at the incident electron energies below 30 eV. These results also include more recent studies of dissociative electron attachment to THF by Sulzer *et al.* [18] and Aflatooni *et al.* [19], who detected anions in two energy regions, around 1.5 eV and between 5 eV and 9 eV.

These scarce experimental works on electron collisions with gaseous THF are accompanied by a number of theoretical *ab initio* calculations published very recently [20–23] which predominantly focus on the low-energy region. Here, Bouchiha *et al.* [20] used the *R*-matrix method to calculate integral elastic and electronically inelastic cross sections in the energy region up to 10 eV. Trevisan *et al.* [21] used the complex Kohn variational method to calculate elastic differential and momentum transfer cross sections in the region up to 20 eV. Winstead and McKoy [22] studied the elastic electron scattering from THF in the energy region up to 50 eV using the Schwinger multichannel method. These authors

 

also investigated the dependence of the elastic scattering on the THF molecular conformation, examining the $C_s$ and $C_2$ geometries and also the planar $C_{2v}$ geometry which was chosen in the calculations of Refs. [20,21]. Finally, Tonzani and Greene [23] calculated elastic integral cross section in the static-exchange-polarization approximation in the energy region up to 20 eV applying the *R*-matrix method. The above theoretical studies predicted the existence of negative ion resonances in the electron THF scattering.

## II. EXPERIMENTAL DETAILS AND PROCEDURES

The present measurements have been performed at Gdańsk University of Technology using a recently constructed hemispherical electron spectrometer. This spectrometer has been described in detail by Linert and Zubek [24]. It consists of a source of incident electron beam, an analyzer of scattered electrons, and a magnetic angle changer. The incident electron beam is produced by a double hemispherical deflector. The molecular beam is formed by effusion of the target gas from a single stainless steel tube with 0.6 mm inner diameter. Electrons scattered from the molecular beam are analyzed by the double hemispherical deflector identical to that used in the electron beam source. The energy resolution of the spectrometer in the present elastic cross-section measurements was typically 70 meV. The incident electron energy is calibrated with an uncertainty of ±30 meV against the monitored position of the $^2P_{3/2}$ negative-ion resonance in argon at 11.098 eV [25]. The scattered electron analyzer can be rotated around the molecular beam axis over angular range from 0° to 90° with respect to the direction of the incident electron beam. The range of accessible scattering angles is further extended into the backward scattering from 90° up to 180° by using the magnetic-angle-changing technique [9–11].

The magnetic angle changer which surrounds the electron scattering center produces a static, localized magnetic field that is perpendicular to the scattering plane [11]. The magnetic field deflects the incident and the scattered electrons. The electrons scattered at the angles from 90° to 180° are detected on the opposite side of the molecular beam with respect to the deflected unscattered beam which is thus well separated from the angular region of electron detection. The scattering angle scale has been calibrated by observing the position of a minimum at 117.5° [26] in the elastic differential cross section of argon at the energy of 10 eV. The uncertainty in the angular scale is ±1.5°. The angular resolution of the spectrometer is estimated from electron optics computational simulations of the transmission of scattered electrons through cylindrical lens of the electron analyzer. It is equal to 2° at 20 eV and increases to 6° at 6 eV.

In the present work differential cross sections for elastic electron scattering from THF have been measured at selected incident electron energies and at scattering angles from 20° to 180° in 10° steps. At a given electron energy, the relative cross section has been derived as a function of scattering angle by measuring the elastic scattering intensity in several overlapping angular regions. The effective scattering volume correction has been applied to the measured intensities from the elastic electron scattering in helium observed under the same experimental conditions as in THF. In the correction the differential cross section of Nesbet [27] has been used, except for 20 eV where the cross section of Saha [28] has been applied. The background contributions which were typically below 10% of the elastic electron intensities have been subtracted from the measured electron yields. The relative cross sections were next normalized to the absolute values obtained at several scattering angles (usually 40° and 140° for each energy) using the relative flow technique [29,30] and procedure described in [31] and again helium as a reference gas with its known differential cross sections [27,28]. The pressure of THF behind the tube forming the molecular beam was maintained below 0.2 mbar. The ratio of the pressures behind the tube for THF to that of helium was adjusted to be 4.6. Here in the determination of the mean free path length for THF in the molecular beam-forming tube the molecular diameter of the THF molecule has been taken to be 4.63 Å. This value has been accepted as an average of the diameter of ethoxy ethane molecule (4.61 Å) [32] which is a linear isomer of THF and tiophene molecule (4.66 Å) [32] which is a five-member ring molecule similar to THF. During the measurements it has been proved by varying the ratio of the helium and THF pressures that absolute values of the cross sections do not depend on the pressure ratio to within uncertainties in the measured cross sections.

In the present studies we have also measured energy dependences of the differential cross sections over limited electron energy ranges for fixed scattering angles. Here, the transmission function of the spectrometer in the elastic scattering mode of operation has been determined from measurements in helium and again using the theoretical differential cross sections of Nesbet [27]. Each energy spectrum has been corrected for variation of transmission with electron energy and normalized to the absolute differential cross sections obtained at the studied scattering angles.

The uncertainties in the presented differential cross sections given as standard deviations are estimated to be 20% at scattering angles of 20° and 30°, 17% at 40°, and 15% in the remaining scattering angle range. These uncertainties result from contributions of statistical uncertainties in the measurements of relative scattered electron intensities (5%) and statistical uncertainties in the measurements of the absolute values of the cross sections and applied normalization procedure (14%). The total uncertainties of the measurements in the 20°–40° scattering angle range, where the cross sections show a step increase with the decreasing scattering angle (characteristic for dipole molecules) also include a contribution due to uncertainty ($<12\%$) in the angular scale calibration (±1.5°). These contributions have been added in quadrature to yield the total uncertainty.

The anhydrous THF was purchased from Aldrich with a declared purity >99.9% and was used after a few freeze-thaw degassing cycles under vacuum. It was introduced into the scattering region from a stainless steel container via a gas line which was heated to a temperature of 45 °C equal to the temperature of the spectrometer. We found that when the gas line was maintained at the room temperature measured flow rate of THF would deviate from the flow rate at the scattering region by as much as 20%.

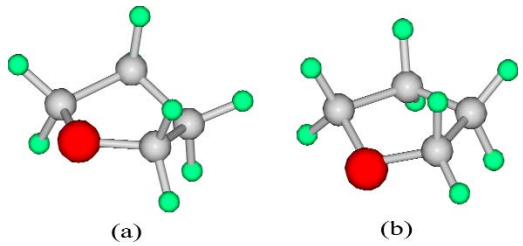


FIG. 1. (Color online) Diagrams of the ground-state equilibrium structures of tetrahydrofuran, $C_4H_8O$, in the (a) $C_2$ (twisted geometry) and (b) $C_s$ (envelope geometry) point symmetry groups. Oxygen atom is red (dark), carbon atom gray (gray), and hydrogen atom green (dark gray).

## III. RESULTS AND DISCUSSION

The THF molecule is a five-member hydrocarbon ring containing an oxygen atom and this structure is incorporated into the deoxyribose sugar. It belongs either to the $C_2$ (twisted geometry) [33] or $C_s$ (envelope geometry) [34] point symmetry groups as shown in Fig. 1. It has a permanent electric-dipole moment of 1.63 D along a symmetry axis through the oxygen atom and a polarizability of 7.97 Å$^3$ [35].

### A. Differential cross sections

Our differential cross sections obtained at electron energies of 6, 7, 8, and 10 eV are shown in Fig. 2, and those obtained at 12, 15, and 20 eV are shown in Fig. 3. The numerical values of the present cross sections are listed in Table I. In the figures our results are compared, at the energies where possible with the very recent measurements of Colyer *et al.* [14] carried out in the scattering angle range from 10° to 130° using the relative flow technique. At the energy of 20 eV they are also compared with the results of Milosavljević *et al.* [13] obtained between 10° and 110°. These figures make also a comparison with the theoretical calculations of Trevisan *et al.* [21] and Winstead and McKoy [22]. These theoretical differential cross sections are in very good agreement with each other for energies between 8 eV and 15 eV, except for the scattering angle range below 10° where the results of Trevisan *et al.* diverge at 0°. At 6 eV, 7 eV, and also at 20 eV these results deviate from each other to some extent; however, they generally show similar angular dependences of the cross sections. In the case of 20 eV an additional comparison is made with the calculations of Blanco and Garcia [36] carried out within the corrected form of the independent-atom method.

At the energies of 6 eV and 7 eV [Figs. 2(a) and 2(b)] calculations of Trevisan *et al.* [21] and Winstead and McKoy [22], overall, are lower than our experimental cross sections. The Schwinger multichannel calculations [22], in the shapes of their angular dependences, are in better agreement with our results than that of Trevisan *et al.* However, the 7 eV theoretical results above 140° are consistently below the experimental cross sections. At 8 eV and 10 eV [Figs. 2(c) and

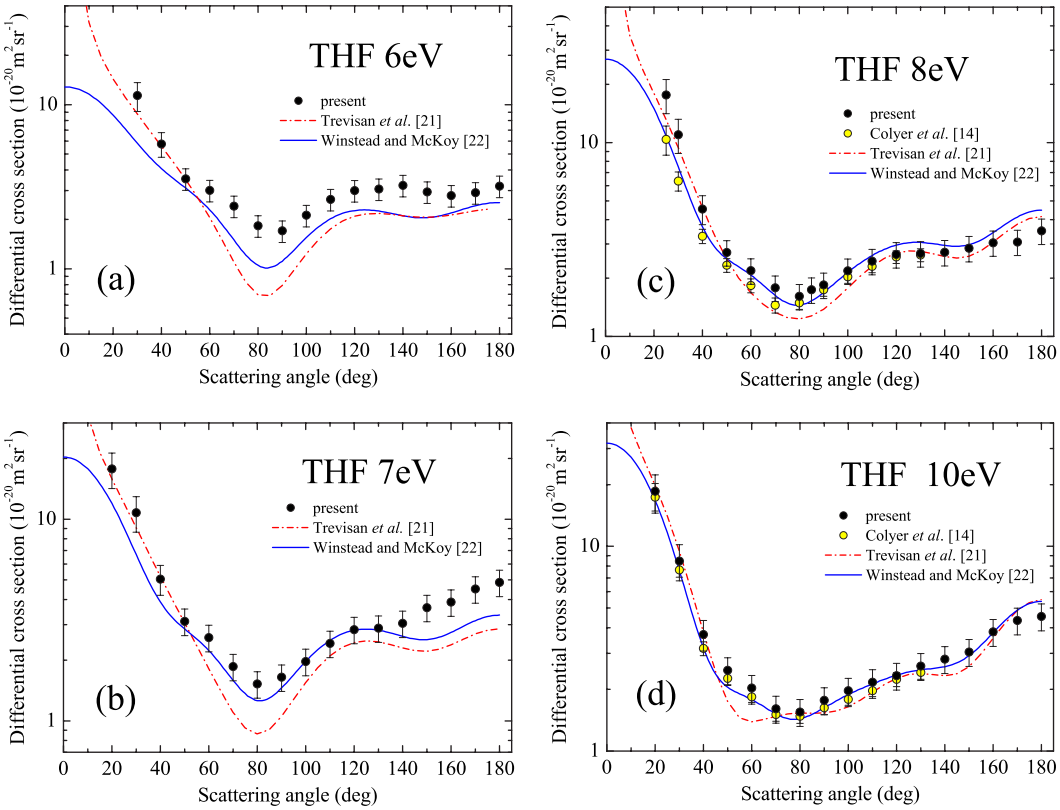


FIG. 2. (Color online) Differential cross sections for elastic electron scattering in tetrahydrofuran at the energy of (a) 6 eV, (b) 7 eV, (c) 8 eV, and (d) 10 eV: (●) present results. In the figures are shown experimental results of Colyer *et al.* [14] and theoretical results of Trevisan *et al.* [21] and Winstead and McKoy [22].

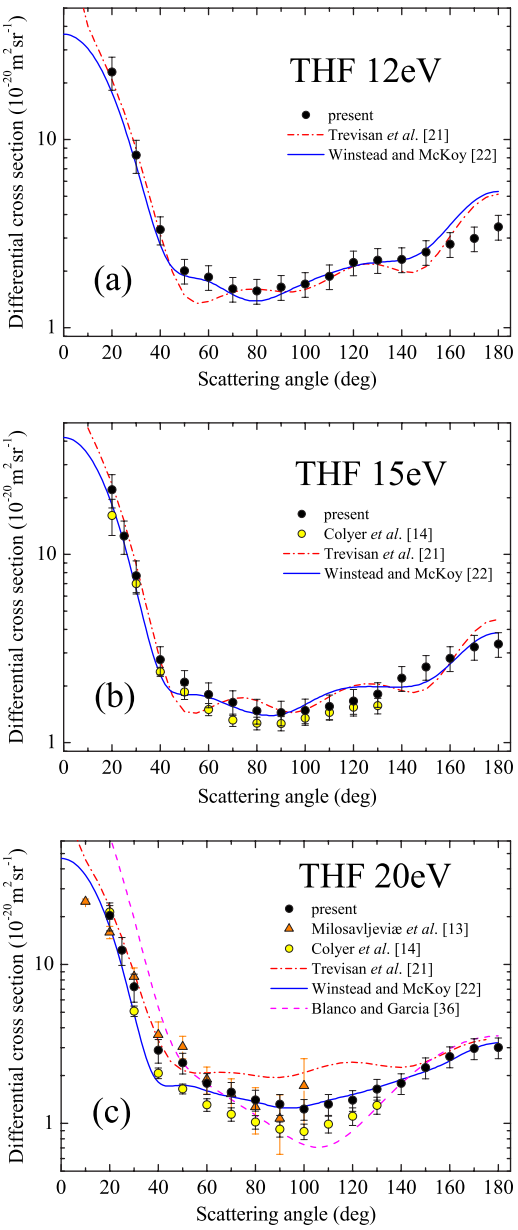


FIG. 3. (Color online) Differential cross sections for elastic electron scattering in tetrahydrofuran at the energy of (a) 12 eV, (b) 15 eV, and (c) 20 eV: (●) present results. In the figures are shown experimental results of Milosavljević *et al.* [13] and Colyer *et al.* [14] and theoretical results of Trevisan *et al.* [21], Winstead and McKoy [22], and Blanco and Garcia [36].

2(d)] the present results are compared with the very recent measurements of Colyer *et al.* [14]. Both measurements are in exceptionally good agreement, deviating only slightly from each other at 8 eV in the region of forward scattering below 40°. The displayed theoretical calculations are in very good agreement with the results of the measurements. In Figs. 3(a) and 3(b) we present results for 12 eV and 15 eV, respectively. Here of note at 15 eV is once more very good agreement between our differential cross section and that of Colyer *et al.* [14]. The calculations of Trevisan *et al.* [21] and Winstead and McKoy [22] agree very well with the experimental cross sections for both energies except at 12 eV in the angular region close to 180°, where the calculated cross sections are substantially above the experimental values. At 20 eV our cross section is compared with the measurements of Colyer *et al.* [14] and those of Milosavljević *et al.* [13]. All three measurements are in relatively good agreement considering the shape of the angular dependence and the absolute values of the cross sections. The results of Winstead and McKoy are in better accordance with our measurements; especially, they coincide with our cross section above about 60°. We have also made a comparison with the independent-atom calculations of Blanco and Garcia [36], which predict the differential cross section for the backward scattering at and above 140° in very good agreement with our experimental results but overestimate the cross section for the forward scattering below 50°.

In these studies, we have also measured differential cross sections as functions of electron energy at fixed scattering angles of 60°, 80°, and 150°. These results are shown in Fig. 4. The elastic scattering functions are in good accordance with the absolute values of the cross sections obtained at selected electron incident energies as shown for the 80° dependence. In these measurements special attention has been paid to the energy region close to the first excitation threshold (6–7 eV), where Bouchiha *et al.* [20] in their calculations which included excited states in the wave function expansion for the target-electron system found narrow Feshbach negative-ion resonances in the elastic cross section. Although the sensitivity of our spectrometer setup allows observation of narrow structures in the cross sections with intensities down to 1% of the scattered electron yields, we failed to see any narrow changes in the cross sections at various scattering angles (Fig. 4). On the other hand, our 80° elastic scattering function shows a weak maximum at about 6 eV and a second wider maximum around 9 eV which both may indicate presence of shape resonances. The 6-eV structure is further confirmed in our 150° function. Similar features of the cross sections are seen in the elastic scattering functions of Colyer *et al.* [14] measured at 60°, 90°, and 120°. Two wider resonance regions between 4 eV and 12 eV can be also discerned in the total cross section measured by Możejko *et al.* [16] (see Fig. 5). They found a sharp rise at 4 eV in their cross section to a maximum at about 6 eV and a second weaker maximum at about 8.5 eV. These maxima in the total cross section may be enhanced by contributions from resonance vibrational excitation of THF. Lepage *et al.* [17] observed a maximum at 8.4 eV in the excitation function of the C-H stretch modes measured in the gas-phase THF and several wide negative-ion resonances located in the 4–10-eV range in the solid phase. In the measurements for the multilayer condensed phase they revealed presence of at least three resonances in the 4–10-eV energy range in the excitation functions for selected vibrational modes. It is finally interesting to note that in the studies of dissociative electron attachment Aflatooni *et al.* [19] detected two processes, at 6.2 eV and 8 eV, leading to the formation of negative ions.

### B. Integral and momentum transfer cross sections

The integral elastic cross section $\sigma_e$ and the momentum transfer cross section $\sigma_m$ have been determined at the elec-

TABLE I. Differential cross sections, in units of $10^{-20}$ m$^2$ sr$^{-1}$, for elastic electron scattering in tetrahydrofuran at incident electron energies of 6, 7, 8, 10, 12, 15, and 20 eV. The uncertainties in the cross sections are 20% at 20° and 30°, 17% at 40°, and 15% in the remaining scattering angle range.

| | Electron energy | | | | | | |
|---|---|---|---|---|---|---|---|
| Scattering angle (deg) | 6 eV | 7 eV | 8 eV | 10 eV | 12 eV | 15 eV | 20 eV |
| 20 | | 17.74 | | 18.58 | 22.86 | 22.09 | 20.36 |
| 25 | | | 17.62 | | | 12.52 | 12.33 |
| 30 | 11.36 | 10.78 | 10.99 | 8.47 | 8.27 | 7.70 | 7.24 |
| 40 | 5.76 | 5.05 | 4.54 | 3.71 | 3.32 | 2.76 | 2.88 |
| 50 | 3.53 | 3.12 | 2.71 | 2.48 | 2.01 | 2.10 | 2.40 |
| 60 | 3.01 | 2.59 | 2.18 | 2.03 | 1.86 | 1.80 | 1.79 |
| 70 | 2.41 | 1.86 | 1.78 | 1.61 | 1.61 | 1.64 | 1.57 |
| 80 | 1.83 | 1.53 | 1.61 | 1.55 | 1.57 | 1.48 | 1.40 |
| 85 | | | 1.74 | | | | |
| 90 | 1.70 | 1.65 | 1.84 | 1.77 | 1.64 | 1.44 | 1.32 |
| 100 | 2.12 | 1.97 | 2.18 | 1.97 | 1.71 | 1.48 | 1.23 |
| 110 | 2.65 | 2.42 | 2.45 | 2.17 | 1.88 | 1.56 | 1.32 |
| 120 | 2.99 | 2.84 | 2.65 | 2.33 | 2.22 | 1.66 | 1.40 |
| 130 | 3.06 | 2.88 | 2.68 | 2.60 | 2.29 | 1.81 | 1.64 |
| 140 | 3.22 | 3.05 | 2.72 | 2.81 | 2.31 | 2.20 | 1.79 |
| 150 | 2.94 | 3.65 | 2.85 | 3.04 | 2.52 | 2.52 | 2.25 |
| 160 | 2.79 | 3.88 | 3.04 | 3.82 | 2.78 | 2.81 | 2.63 |
| 170 | 2.91 | 4.51 | 3.07 | 4.34 | 2.98 | 3.23 | 2.96 |
| 180 | 3.19 | 4.86 | 3.51 | 4.55 | 3.44 | 3.34 | 3.00 |

tron energies of the present work from numerical integration of the differential cross sections over the total scattering angle range 0°–180°. For the 0°–20° angular range the present cross sections have been extrapolated down to 0° using the theoretical cross sections of Winstead and McKoy [22]. These cross sections have been multiplied by a constant to coincide with our experimental cross sections at 30°. We note here that these theoretical cross sections show good agreement with our measurements in the shape of the angular behavior in the 20°–40° angular range for all present electron incident energies except 6 eV. Here we have normalized the calculated cross section to an average experimental value for 20° and 30°. The deduced integrated cross sections are listed in Table II. The uncertainties in the integral cross section and the momentum transfer cross section are estimated to be 18%

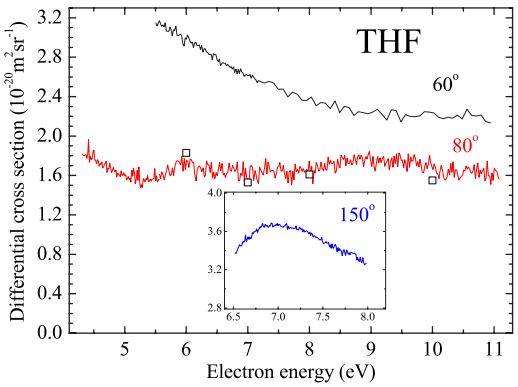


FIG. 4. (Color online) Differential cross sections for elastic electron scattering in tetrahydrofuran in the energy range from 4.5 eV to 11 eV and at the scattering angles of 60°, 80°, and 150°. The squares show absolute values of the differential cross sections obtained at 80° in the measurements at fixed electron energies.

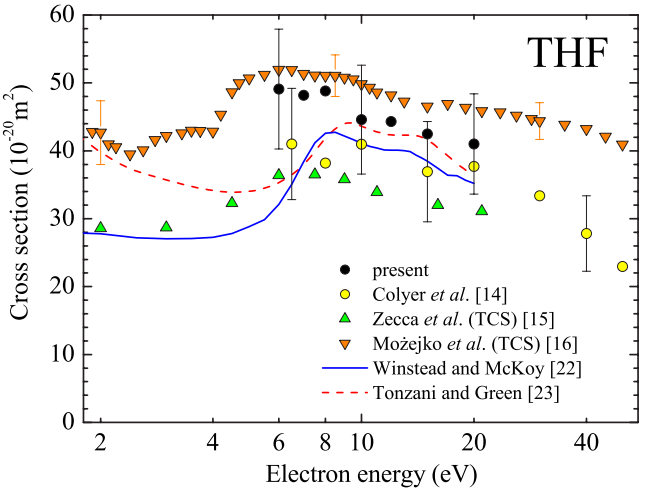


FIG. 5. (Color online) Integral cross sections for elastic electron scattering in tetrahydrofuran: (●) present results. In the figure are shown experimental results of Colyer *et al.* [14], total cross section results of Zecca *et al.* [15] and Możejko *et al.* [16], and theoretical results of Winstead and McKoy [22] and Tonzani and Greene [23].

TABLE II. Integral cross section $\sigma_e$ and momentum transfer cross section $\sigma_m$, in units of $10^{-20}\,m^2$, for elastic electron scattering in tetrahydrofuran at incident energies of 6, 7, 8, 10, 12, 15, and 20 eV. The uncertainties in the integral and momentum transfer cross sections are 18% and 16%, respectively.

| Energy (eV) | $\sigma_e$ | $\sigma_m$ |
|---|---|---|
| 6 | 49.1 | 34.6 |
| 7 | 48.2 | 34.9 |
| 8 | 48.8 | 32.0 |
| 10 | 44.6 | 31.4 |
| 12 | 44.3 | 28.7 |
| 15 | 42.5 | 25.2 |
| 20 | 41.0 | 22.4 |

and 16%, respectively. The extrapolated cross sections of the 0°–20° range, which we have attributed an uncertainty of 20% equal to that of 20° differential cross sections, introduce 25% and less than 1% contributions to the final uncertainties of the integral and momentum transfer cross sections, respectively. We have also found that the differential cross sections below 50°, with their steep increase with decreasing scattering angle, introduce a 55% contribution to the integral elastic cross sections but a much lower contribution, of 8%, to the momentum transfer cross sections.

The deduced integral and momentum transfer cross sections are presented in Figs. 5 and 6, respectively, together with those determined by Colyer *et al.* [14] from their differential cross-section measurements and obtained in theoretical calculations [21–23]. The integral cross sections are also compared with the measured total cross sections [15,16] (Fig. 5). Our integral elastic cross section decreases with increasing energy in agreement with the tendency shown in the 6–20-eV energy range by the total cross section of Możejko *et al.* [16]. It is in overall agreement with the determination of that cross section by Colyer *et al.* [14], although our values of the cross section in the 6–8-eV range seem to be slightly higher than those of Colyer *et al.* Our preliminary determination of the total integral vibrational

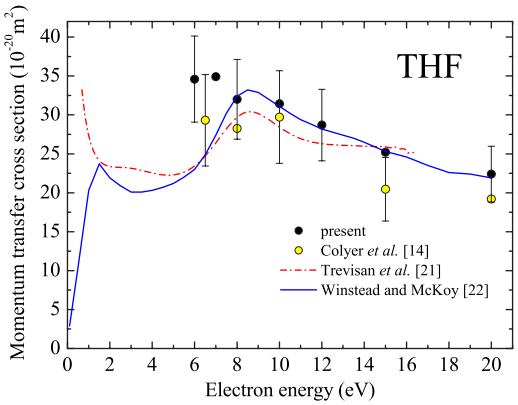


FIG. 6. (Color online) Momentum transfer cross sections in tetrahydrofuran: (●) present results. In the figure are shown experimental results of Colyer *et al.* [14] and theoretical results of Trevisan *et al.* [21] and Winstead and McKoy [22].

cross section at 7 eV which includes vibrational modes observed in the energy loss spectra [12] gave a value of $5.0 \times 10^{-20}\,m^2$ which when added to our integral elastic cross section gives total cross section of $53.2 \times 10^{-20}\,m^2$. This value coincides very well with the total cross section of Możejko *et al.* ($51.3 \times 10^{-20}\,m^2$). The electronic excitation of the THF at this energy is very weak, and the dissociative electron attachment cross section is equal to about $10^{-24}\,m^2$ [19].

The Schwinger multichannel calculations of Winstead and McKoy [22] predict the presence of overlapping shape resonances in the integral cross section with a peak at about 8.3 eV and in addition found a resonance related shoulder between 13 eV and 14 eV. These calculations have been conducted for $C_2$ conformation of the THF and included configurations built on excited target configurations. Also the *R*-matrix calculations of Tonzani and Greene [23] revealed two broad resonances at about 8.6 eV and 14.1 eV in accordance with the calculation of Winstead and McKoy [22]. A resonance maximum at about 8.5 eV, however, is not borne out by the experimental integral cross sections (Fig. 5). This fact may indicate that although both calculations predict shape resonances generating a maximum in the cross section in the 8.3–8.6-eV energy region, they do not reproduce a resonance at 6 eV, which stems from the present experimental work, that of Colyer *et al.* [14] and total cross- section measurements. Above the maximum the theoretical cross sections agree well with the experimental values.

Figure 6 shows a comparison of the present momentum transfer cross section with that of Colyer *et al.* [14] and with the results of the calculations [21,22]. Trevisan *et al.* [21] in their calculations, which were restricted to electronically elastic scattering, reported the presence of a broad resonance feature in the momentum transfer cross section at about 8.6 eV which is a result of two overlapping shape resonances of $A_1$ and $B_2$ symmetries. The momentum transfer cross section calculated by Winstead and McKoy [22] agrees very well with that of our determination down to about 8 eV. Both theoretical cross sections show maxima at about 8.5 eV in contrast to our cross section which below 8 eV slightly increases. Similar energy behavior of the cross section below 8 eV is shown by the results of Colyer *et al.* The momentum transfer cross section, from its definition, includes a higher contribution from the high angle scattering. For the present case of THF it would suppress the contribution of forward scattering due to electron-dipole interaction in favor of interactions leading to resonance scattering. The higher momentum transfer cross section at about 6 eV is further supporting presence of a resonance in this energy region.

## IV. CONCLUSIONS

In the present work we have measured absolute differential cross sections for elastic electron scattering at the selected values of electron energies in the 6–20-eV range and over continuous scattering angle range from 20° to 180°. We have compared our results with the very recent complex Kohn variational calculations of Trevisan *et al.* [21] and the Schwinger multichannel calculations of Winstead and

McKoy [22]. Both theoretical calculations are in very good agreement with the present measurements in the energy range from 8 eV to 15 eV, but at 6 eV and 7 eV are generally lower than the present measurements. We have also studied differential cross sections for elastic scattering as a function of electron energy for fixed scattering angles. These elastic scattering functions reveal two energy regions, at about 6 eV and around 9 eV of resonance scattering via wide, shape resonances.

The differential cross sections have been integrated over the complete scattering angle range 0°–180° to obtain integral and momentum transfer cross sections. The theoretical integral cross sections [22,23] are in good and the momentum transfer cross sections [21,22] are in very good agreement with the presently deduced cross sections in the energy region above about 8 eV. However, our experimental cross sections do not confirm the theoretically predicted resonance maxima in the cross sections at about 8.5 eV. The deduced integral elastic cross section allowed us additionally to clear the inconsistences in the total cross-section measurements in THF in favor of the results of Możejko *et al.* [16].

## ACKNOWLEDGMENTS

We are grateful to Cynthia Trevisan, Carl Winstead, Gustavo Garcia, and Stefano Tonzani for providing their calculated cross sections in numerical form and also to Stephen Buckman for sending his experimental results prior to publication. This work has been carried out within the European Science Foundation program "Electron Induced Processing at the Molecular Level" (EIPAM). One of us (A.R.M.) acknowledges the European Science Foundation for support through the EIPAM programme. This work was also partly supported by the Polish State Committee for Scientific Research and by MSEP of Serbia under Project No. 141011.

[1] B. Boudaiffa, P. Cloutier, D. Hunting, M. A. Huels, and L. Sanche, Science **287**, 1658 (2000).
[2] L. Sanche, Eur. Phys. J. D **35**, 367 (2005).
[3] G. Hanel, B. Gstir, S. Denifl, P. Scheier, M. Probst, B. Farizon, M. Farizon, E. Illenberger, and T. D. Märk, Phys. Rev. Lett. **90**, 188104 (2003).
[4] H. Abdoul-Carime, S. Gohlke, and E. Illenberger, Phys. Rev. Lett. **92**, 168103 (2004).
[5] C. Winstead and V. McKoy, J. Chem. Phys. **125**, 244302 (2006).
[6] R. Abouaf, J. Pommier, and H. Dunet, Chem. Phys. Lett. **381**, 486 (2003).
[7] A. Roldán, J. M. Pérez, A. Williart, F. Blanco, and G. Garcia, J. Appl. Phys. **95**, 5865 (2004).
[8] J. C. Oller, A. Munoz, J. M. Peréz, F. Blanco, P. Limao-Viera, and G. Garcia, Chem. Phys. Lett. **421**, 439 (2006).
[9] M. Zubek, N. Gulley, G. C. King, and F. H. Read, J. Phys. B **29**, L239 (1996).
[10] F. H. Read and J. M. Channing, Rev. Sci. Instrum. **67**, 2372 (1996).
[11] I. Linert, G. C. King, and M. Zubek, J. Electron Spectrosc. Relat. Phenom. **134**, 1 (2004).
[12] A. R. Milosavljević, I. Linert, M. Dampc, B. P. Marinković, and M. Zubek, in *Proceedings of the 23rd International Symposium on the Physics of Ionized Gases, Kopaonik, Serbia, 2006*, edited by N. S. Simonović, B. P. Marinković, and Lj. Hadzievski (Institute of Physics, Belgrade, 2006), p. 37.
[13] A. R. Milosavljević, A. Giuliani, D. Šević, M.-J. Hubin-Franskin, and B. P. Marinković, Eur. Phys. J. D **35**, 411 (2005).
[14] C. J. Colyer, V. Vizcaino, J. P. Sullivan, M. J. Brunger, and S. J. Buckman, New J. Phys. **9**, 41 (2007).
[15] A. Zecca, Ch. Perazzolli, and M. J. Brunger, J. Phys. B **38**, 2079 (2005).
[16] P. Możejko, E. Ptasińska-Denga, A. Domaracka, and C. Szmytkowski, Phys. Rev. A **74**, 012708 (2006).
[17] M. Lepage, S. Letarte, M. Michaud, F. Motte-Tollet, M.-J. Hubin-Franskin, D. Roy, and L. Sanche, J. Chem. Phys. **109**, 5980 (1998).
[18] P. Sulzer, S. Ptasińska, F. Zappa, B. Mielewska, A. R. Milosavljević, P. Scheier, T. D. Maerk, I. Bald, S. Gohlke, M. A. Huels, and E. Illenberger, J. Chem. Phys. **125**, 044304 (2006).
[19] K. Aflatooni, A. M. Scheer, and P. D. Burrow, J. Chem. Phys. **125**, 054301 (2006).
[20] D. Bouchiha, J. D. Gorfinkiel, L. G. Caron, and L. Sanche, J. Phys. B **39**, 975 (2006).
[21] C. S. Trevisan, A. E. Orel, and T. N. Rescigno, J. Phys. B **39**, L255 (2006).
[22] C. Winstead and V. McKoy, J. Chem. Phys. **125**, 074302 (2006).
[23] S. Tonzani and C. H. Greene, J. Chem. Phys. **125**, 094504 (2006).
[24] I. Linert and M. Zubek, J. Phys. B **39**, 4087 (2006).
[25] J. N. H. Brunt, G. C. King, and F. H. Read, J. Phys. B **10**, 1289 (1977).
[26] J. C. Gibson, R. J. Gulley, J. P. Sullivan, S. J. Buckman, V. Chan, and P. D. Burrow, J. Phys. B **29**, 3177 (1996).
[27] R. K. Nesbet, Phys. Rev. A **20**, 58 (1979).
[28] H. P. Saha, Phys. Rev. A **40**, 2976 (1989).
[29] M. A. Khakoo and S. Trajmar, Phys. Rev. A **34**, 138 (1986).
[30] J. C. Nickel, C. Mott, I. Kanik, and D. C. McCollum, J. Phys. B **21**, 1867 (1988).
[31] I. Linert, G. C. King, and M. Zubek, J. Phys. B **37**, 4681 (2004).
[32] *Landolt-Börnstein, Zahlenwerte und Funktionen, Bd I, Atom und Molekularphysik, 1, Atome und Ionen*, edited by A. Eucken (Springer-Verlag, Berlin, 1950).
[33] B. Cadioli, E. Gallinella, C. Coulombeau, H. Jobic, and G. Berthier, J. Phys. Chem. **97**, 7844 (1993).
[34] V. M. Rayón and J. A. Sordo, J. Chem. Phys. **122**, 204303 (2005).
[35] National Institute of Standards and Technology, http://srdata.nist. gov/cccbdb/alldata2.asp?casno=109999
[36] F. Blanco and G. Garcia (private communication).